Synthesis, Characterization, and Theoretical Study of a New Organotellurium Ligands Containing Amino Group

Gofran Safi Mokhtar[1] and Nuha Hussain Al-Saadawy[2*]

[1]*Faculty of Archaeology, University of Thi-Qar, Thi-Qar, 64001, Iraq*

[2]*Department of Chemistry, College of Science, University of Thi-Qar, Thi-Qar, 64001, Iraq*

* ***Corresponding author:***

email: nuh.hussain@sci.utq.edu.iq

Received: June 20, 2022
Accepted: August 2, 2022

DOI: 10.22146/ijc.75583

Abstract: *The aim of the current study is to prepare organomercury and organotellurium compounds containing amino groups such as [1,1'-biphenyl]-4-amine and their derivatives by a mercuriation reaction. The research includes the preparation of a new organotellurium compound based on [1,1'-biphenyl]-4-amine. $C_{12}H_{10}NHgCl$ (A) was obtained by mercuriation reaction to [1,1'-biphenyl]-4-amine by mercuric acetate and lithium chloride. $C_{12}H_{10}Br_3NTe$ (B), $C_{24}H_{20}N_2Br_2Te$ (C), $C_{24}H_{20}N_2Te$ (D), and $C_{24}H_{20}N_2Te_2$ (E) were prepared by different reactions to get the corresponding compounds. All the prepared ligands were characterized by using infrared spectroscopy and mass spectroscopy. DFT has been obtained by the basis set 3-21G to investigate the molecular structure of the new prepared organotellurium compounds. HOMO and LUMO surfaces, geometrical structure, and energy gap have been obtained throughout the geometry optimization. Finally, the electron affinity, electronegativity, electrophilicity, ionization potential, and lower case of organotellurium compounds have been calculated and discussed. The result of the chemical analysis showed that it agreed with the proposed chemical structures, and a theoretical study using DFT has concluded that more stability of the prepared organotellurium compounds.*

Keywords: *organotellurium; 4-amino biphenyl; ditelluride; organyl tellurium dibromide*

■ INTRODUCTION

Tellurium belongs to the family of chalcogens in the sixth group of the periodic table, which is the oxygen group itself. It is a metalloid with atomic number 52 and has five known oxidation states -1, -2, +2, +4, and +6 [1]. Tellurium is a toxic element, but it has existed in the human diet, where it is used in some side metabolic processes [2]. The low natural abundance of the element tellurium has partly been reflected in the scant interest attached to it. Based on old studies, the structures and reactions of tellurium compounds can be extrapolated by studying the behavior of analogs of other lighter chalcogens such as Sulfur and Selenium. In fact, recent results and well-established observations clearly show that this assumption or concept is invalid; the emerging importance of the unique properties of tellurium compounds from a variety of their known and potential applications in both inorganic and organic chemistry [3-4]. Tellurium is derived from the Latin word *tellus*, which means earth, and was discovered by the scientist, Reichenstein, in 1782 from ores extracted from the gold regions of Transylvania [5-6]. For the element tellurium, there are a number of stable isotopes, of which there are eight stable isotopes (Te-120, Te-122, Te-123, Te-124, Te-125, Te-126, Te-128, and Te-130) in addition to twenty-one synthetic isotopes that take the cluster shape in their structures [7-8]. Despite the relative abundance of tellurium in the human body, nevertheless, the diverse activities of tellurium agents in both cancerous and normal cells are important, though highly complex [2,9]. The element tellurium is similar to selenium in terms of its structural formula, but it has a more distinct metallic character than selenium. It has an anisotropic crystalline structure consisting of long helical chains of atoms

arranged symmetrically, each atom having four bonds with its nearest neighbors in adjacent chains [10]. Tellurium is a great significant element for research purposes in the modern era of its entry into the manufacture of nano-devices [11-12]. Tellurium compounds are also used in the field of the plastics and rubber industry to add hardness to electronic industries, optics, and the ceramics industry. Also, it is utilized in petroleum refining and petrochemical industries. Other uses of tellurium are in the manufacture of crackers and fireworks as an explosive material [13-15].

In this work, we synthesized a new organometallic compound type organomercury and organotellurium namely (4-amino-[1,1'-biphenyl]-3-yl)mercury(II) chloride hereinafter referred to as compound **A**, 3-(tribromo-λ^4-tellanyl)-[1,1'-biphenyl]-4-amine hereinafter referred to as compound **B**, 3,3'-(dibromo-λ^4-tellanediyl)bis([1,1'-biphenyl]-4-amine) hereinafter referred to as compound **C**, 3,3''-tellurobis([1,1'-biphenyl]-4-amine) hereinafter referred to as compound **D**, and 3,3''-ditellanediyl bis([1,1'-biphenyl]-4-amine) hereinafter referred to as compound **E**, then the molecular structure of organotellurium compound (**B**–**E**) has been investigated theoretically by the DFT with a good agreement of theoretical results.

■ EXPERIMENTAL SECTION

Materials

The chemicals used in this study included ethanol absolute, bromine, sodium metal, lithium chloride (Sigma-Aldrich), glacial acetic acid, mercuric acetate, hydrazine hydrate, dioxane (Fluka), chloroform, potassium hydroxide, tellurium powder (BDH), hydrochloric acid (HGB).

Instrumentation

Infra-red spectra were recorded with KBr disks utilizing an FTIR spectrophotometer Shimadzu model 8400 S in reach 4000–250 cm^{-1}. The mass spectra were performed using a HAT-8200 analyzer at the ionizing potential of 70 eV (Central Laboratory, University of Tehran, Iran). The melting point was measured using the Melting point SMP 31 model.

Procedure

Synthesis of (4-amino-[1,1'-biphenyl]-3-yl)mercury(II) chloride (A)

Firstly, 8.3 g (0.05 mol) of 4-amino biphenyl was dissolved in 50 mL of absolute ethanol, then added to it 15.7 g (0.05 mol) of mercury acetate dissolved in 50 mL of absolute ethanol, and the mixture was refluxed for 12 h with the follow-up of the reaction via thin-layer chromatography TLC. After the reaction was completed, 2.5 g (0.06 mol) of lithium chloride was added, and the reaction was continued again for 1 h then the solution was filtered. White crystals were formed on the filter paper and then washed via hot ethanol several times to get rid of the remains of unwanted materials. The weight of produced compound was 15.3 g, the yield was 77%, and the melting point of the compound was measured after completely drying was 170–172 °C.

FT-IR using KBr: ν(C–H) Aromatic = 3055 cm^{-1}, ν(C–N) Aromatic = 1310 cm^{-1}, ν(C=C) Aromatic = 1612 cm^{-1}, ν(NH_2) = (3327 cm^{-1}, 3408 cm^{-1}).

Mass spectra: The MS calculated for **A** $C_{12}H_{10}NHgCl$ (404.26) was found to be as follows: M^++1 (405); MS/MS (*m/z*): 365, 317, 277, 236, 169, 154, 144, 78.

These data were shown in Scheme 1 and S1, Table 1, 2 and S1, Fig. S1, S2 and S3.

Synthesis of 3-(tribromo-λ⁴-tellanyl)-[1,1'-biphenyl]-4-amine (B)

Add 16 g of compound **A** with 18 g (0.04 mol) of $TeBr_4$ and both materials in their solid state after grinding them well (the reaction here was at a ratio of 1:1 mole, then add 400 mL of glacial acetic acid. The mixture was refluxed for 15 h, and the reaction progress was followed up by TLC to assure the completion of the reaction. In the first hours of the reaction, the color of the solution turns brown, and after the end of the heating period, we filter the solution under hot conditions. The filtered mixture then has left to cool down, where we notice the formation of dark brown crystals that are the compound 3-(tribromo-λ^4-tellanyl)-[1,1'-biphenyl]-4-amine to be prepared; separated by normal filtration. The precipitate was washed on a filter paper with hot ethanol, and the precipitate was dried and collected. The weight of produced compound was 13 g,

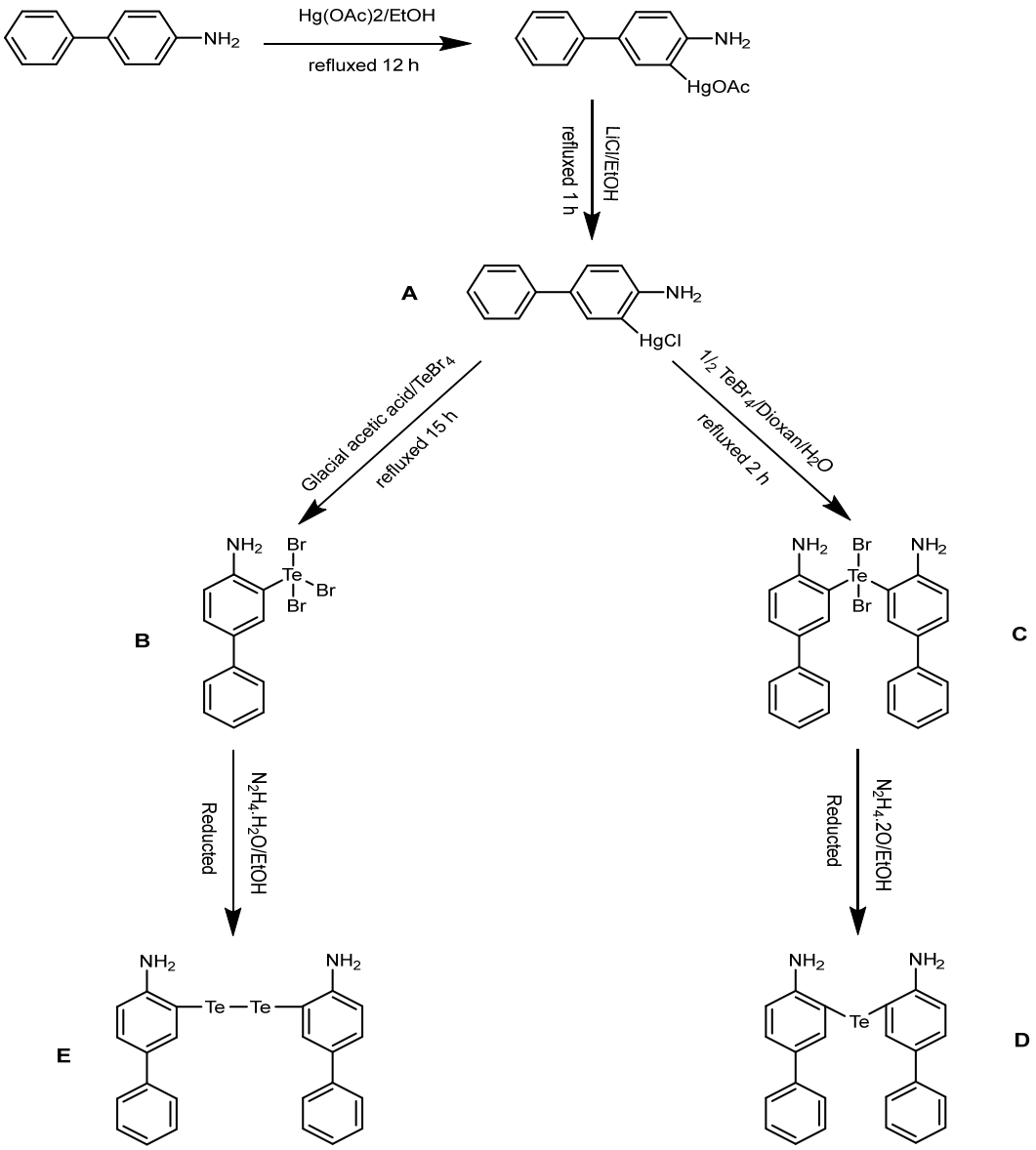

Scheme 1. Synthesis of organotellurium compounds **A**-**E**

and the yield was 60%. The dissociation of the compound was at a degree 161–163 °C.

FT-IR using KBr: ν(C–H) Aromatic = 3121 cm^{-1}, ν(C–N) Aromatic = 1256 cm^{-1}, ν(C=C) Aromatic = 1596 cm^{-1}, ν(NH_2) = (3486 cm^{-1}, 3576 cm^{-1}), ν(C–Te) = 481 cm^{-1}, ν(Br–Te) = 689 cm^{-1}.

Mass spectra: The MS calculated for **B** $C_{12}H_{10}Br_3NTe$ (535.53) was found to be as follows: M^++1 (536); MS/MS (*m/z*): 510, 456, 484, 375, 202, 196, 169.

These data were shown in Scheme 1 and S2, Table 1, 2 and S2, Fig. S4, S5 and S6.

Synthesis of 3,3'-(dibromo- λ ⁴-tellanediyl)bis([1,1'-biphenyl]-4-amine) (C)

Five grams (0.013 mol) of **A** with 2.7 g (0.006 mol) of $TeBr_4$ were mixed, and both materials in their solid state after grinding them well (the reaction here is 2:1 mole). Then 50 mL of dry dioxane was added, and after the process of re-escalation for 2 h, we filtered the mixture while it was hot and left the filtrate to cool down to room temperature. It has noticed the separation of white crystals resembling glass fragments which is the complex (HgClBr.dioxan), and we get rid of them by

Table 1. Physical data for organotellurium compounds

Compound	Molecular formula	M.Wt	Color	m.p. (°C)	Yield (%)
A	$C_{12}H_{10}ClHgN$	404.26	white	170–172	77
B	$C_{12}H_{10}Br_3NTe$	535.53	dark brown	161–163	60
C	$C_{24}H_{20}Br_2N_2Te$	623.85	pale yellow	182–184	50
D	$C_{24}H_{20}N_2Te$	464.04	pale green	208–210	42
E	$C_{24}H_{20}N_2Te$	591.64	orange	214–216	32

Table 2. Main absorption bands in the infrared spectra of the prepared compounds

Compound	C-H aromatic (cm^{-1})	C=C (cm^{-1})	N-H_2 (cm^{-1})	Te-Br (cm^{-1})	C-N (cm^{-1})	Te-c (cm^{-1})
A	3055	1612	3408, 3327	-	1310	-
B	3121	1596	3486, 3573	689	1256	481
C	3033	1609	3582, 3523	692	1284	455
D	3032	1480	3298, 3442	-	1261	499
E	3045	1564	3478, 3567	-	1258	478

normal filtration, then adding the filtrate in batches to 300 mL of ice-distilled water in a beaker with continuous stirring, where we have crystals with the pale color yellow is isolated by filtering. The precipitate was washed on the filter paper with distilled water several times, and the precipitate was dried; the resulting weight is 4 g, and the yield was 50%. The dissociation of the compound at a degree 182–184 °C.

FT-IR using KBr: ν(C–H) Aromatic = 3033 cm^{-1}, ν(C–N) = 1284 cm^{-1}, ν(C=C) Aromatic = 1609 cm^{-1}, ν(NH_2) = (3582 cm^{-1}, 3523 cm^{-1}), ν(C–Te) = 455 cm^{-1}, ν(Br–Te) = 692 cm^{-1}.

Mass spectra: The MS calculated for **C** $C_{24}H_{20}N_2Br_2Te$ (623.85) was found to be as follows: M^++2 (625); MS/MS (*m/z*): 608, 593, 484, 434, 360, 281, 154.

These data were shown in Scheme 1 and S3, Table 1, 2, and S3, Fig. S7, S8 and S9.

Synthesis of 3,3''-tellurobis([1,1'-biphenyl]-4-amine) (D)

From the previously prepared composite, compound **C**, 1 g was dissolved in a beaker and then added 20 mL of ethanol, then some drops of (0.1 mol, 5 mL) of aqueous hydrazine diluted in 5 mL of ethanol were added until the vapors disappear. Pale green crystals were formed and isolated by filtration. The precipitate is washed with hot ethanol on the filter paper and dried, where the resulting weight was 0.3 g, and the yield was 46%. The dissociation of the compound at a degree 208–210 °C.

FT-IR using KBr: ν(C–H) Aromatic = 3032 cm^{-1}, ν(C–N) Aromatic = 1261 cm^{-1}, ν(C=C) Aromatic = 1480 cm^{-1}, ν(NH_2) = (3298 cm^{-1}, 3442 cm^{-1}), ν(C–Te) = 499 cm^{-1}.

Mass spectra: The MS calculated for **D** $C_{24}H_{20}N_2Te$ (464.02) was found to be as follows: M^++2 (466); MS/MS (*m/z*): 449, 415, 364, 296, 169, 154, 78.

These data were shown in Scheme 1 and S4, Table 1, 2 and S4. Fig. S10, S11 and S12.

Synthesis of 3,3''-ditellanediyl bis([1,1'-biphenyl]-4-amine) (E)

From the previously prepared composite, compound **B**, 1 g was put in a beaker, then added 20 mL of ethanol until got completely dissolved in the solvent after heating. Some drop 5 mL (0.1 mol) of aqueous hydrazine diluted in 5 mL of ethanol were added until the fumes disappeared where orange crystals are formed that are isolated by filtration. The precipitate was washed with hot ethanol on a filter paper. The resulting weight was 0.32 g, and the yield was 32%. The dissociation of the compound was at a degree 214–216 °C.

FT-IR using KBr: ν(C–H) Aromatic = 3045 cm^{-1}, ν(C–N) = 1258 cm^{-1}, ν(C=C) Aromatic = 1564 cm^{-1}, ν(NH_2) = (3478 cm^{-1}, 3567 cm^{-1}), ν(C–Te) = 478 cm^{-1}.

Mass spectra: The MS calculated for **E** $C_{24}H_{20}N_2Te_2$ (591.64) was found to be as follows: M^++1 (592); MS/MS (*m/z*): 576, 552, 504, 478, 296, 169, 93.

These data were shown in Scheme 1 and S5, Table 1, 2 and S5, Fig. S13, S14 and S15.

■ RESULTS AND DISCUSSION

This current study included the preparation of the organic tellurium compounds such as $ArTeBr_3$, Ar_2TeBr_2, Ar_2Te, and Ar_2Te_2, where Ar is the organic compound (4-amino biphenyl), which represents the organic part in the prepared organic tellurium compounds, Scheme 1.

IR spectra of the compounds under study displayed standard features in specific regions and characteristic bands in the other areas explained in Table 2. In all the compounds under study, the aromatic C–H bond appeared in the range 3032–3121 cm^{-1} [16-21]. The clear band in the range of 1480–1612 cm^{-1} was attributed to the aliphatic bond C=C [16-21]. A clear double package also appeared in all the compounds prepared, belonging to the NH_2 group within the range 3298–3573 cm^{-1} [16-20]. The appearance of a weak to medium intensity band in the fingerprint area for the two compounds **B** and **C** are 689 and 691 cm^{-1} straight, belonging to the Br-Te bond [17,22-25]. All compounds except **A** showed a weak to medium intensity band within the range 481–499 cm^{-1} belonging to the Te-C bond [17-21], while those spectra which showed bands at 1256–1310 cm^{-1} are due to the amplitude oscillation of the C–N bond [26-27].

The mass spectrum gives clear evidence about the formula of the proposed compounds by noting the value of the molecular ion, the parent band, which refers to the total molecular weight of the compound, in addition to the baseband with high abundance, which indicates the high stability of the fragmented molecule, and that the presence of other bands gives us an idea of the structural formula and the possibility of ions that depend on the rules of fragmentation [28-32]. (Explained in Table 2 and S1–S5, Scheme S1–S5, and Fig. S1-S15).

Computational Study

The molecular structure for the organotellurium compounds was investigated using optimization plus frequency at the ground state level. In addition, density functional theory has been applied to optimize the organotellurium compounds with Gaussian 09 software program [33-39].

Density Functional Theory (DFT)

It is one of the methods used in the study of molecular structures, electronic properties, and lines the circumference and surfaces of individual atoms and molecules, and this method is widely used in science materials and Solid-State Physics. DFT theory deals with electron density rather than the wave function. That is, the electron density depends only on the spatial coordinates without regard to how it is located electrons in the system [32]. DFT is one of the most important methods; it is used in theoretical physics and chemistry, and with it, we can determine the properties of multiple system particles (total system energy, electron density of orbitals, physical, and optical parameters for matter), which is one of the most widely used methods in quantitative calculations because of the possibility of it applied to a variety of systems at a low cost and high speed [34-35].

Electronic Properties

HOMO and LUMO are terms used to refer to the position of molecular orbitals in terms of it is occupied with electrons, as HOMO is the highest molecular orbital occupied by electrons, and LUMO represents the lowest unoccupied molecular orbital with electrons (see Fig. S16–S27). Uses the energy difference between these two boundary orbits in knowing the stability and stability of the elements in addition to the color that they show in solutions (energy gap). The energy gap is the amount of energy needed for an electron to move from its valence level to its conductivity level through this value (energy gap). We can know what elements or materials are if it is a conductor, an insulator, or a semiconductor, where the energy gap can be calculated by difference. The energy between the lowest energy level and the highest energy level [36-37], represents the energy difference between the lower virtual energy and the higher total energy levels (see Table 3).

$$E_g = E_{LUMO} - E_{HOMO} \quad [38] \ (1)$$

The HOMO and LUMO energies are explained in Table 3. The HOMO energy of prepared compounds

Table 3. The electronic states of the organotellurium compounds

Compound	E_{HOMO} (eV)	E_{LUMO} (eV)	E_g (eV)
$RTeBr_3$ (**B**)	5.4011	2.9767	2.4244
R_2TeBr_2 (**C**)	4.3454	2.6230	1.7224
R_2Te (**D**)	4.4814	3.3876	1.0938
R_2Te_2 (**E**)	4.9821	2.5522	2.4299

were arranged [34-38] as follows:

C > **D** > **E** > **B**

while the LUMO energies were arranged as the following [34-38]:

E > **C** > **B** > **D**

Therefore, the highest energy gap was observed by compound **E**, while the lowest value was observed by compound **D** (see Table 3).

Electronegativity and Electrophilicity

Electronegativity is defined as the ability of an atom to attract electrons towards itself in a chemical compound, where fluorine is the most negative electrolyte element. Electronegativity increases with increasing numbers of atomic elements. In addition, electronic affinity can be defined as the susceptibility of a neutral atom. In the gaseous state, it can gain one electron and release energy; the atomic number becomes more difficult to add an electron. Electronegativity and electronic affinity can be calculated respectively from the two relationships (2) and (3) [38-39] as shown in Table 4.

$$X = \frac{E_{HOMO} + E_{LUMO}}{2} \quad (2)$$

$$W = \frac{X^2}{2\eta} \quad (3)$$

In Table 4, the electronegativity of organotellurium compounds under study was arranged as the following:

D > **B** > **C** > **E**

but compound **E** had the greatest electrophilicity, whereas compound **D** had the least such as the following arrangement:

E > **C** > **B** > **D**

Ionization potential and electron affinity ionization energy are defined as the amount of energy required to remove an electron from an atom of a particular element. It is neutral in its gaseous state; for example, a hydrogen atom has one ionization energy in the outer shell because it has one electron, while atoms that contain more than an electron in their last shell have ionization energy for each electron, while electronic affinity can be defined as it is the amount of energy released when an atom gains an electron equal to the energy required to remove an electron from a negative ion. For example, atoms have seven electrons in the outer shell. It has a strong electronegativity, and it is opposite, if the atoms have a closed shell, then they have an attraction weak electronic, and according to Koopman's theory, the following Eq. (4) and (5) [18,28,37-38] can express the ionization potential and electron affinity, as shown in Table 5.

$$I.P = -E_{HOMO} \quad (4)$$

$$E.A = E_{LUMO} \quad (5)$$

The information in Table 5 shows the ionization potentials and electron affinity values in (eV) for compounds **B**, **C**, **D**, and **E**. According to Koopman's theory, the results of ionization potentials and electron affinity, in turn, depend on the energies in the valence band and conduction distance preserver; accordingly, the prepared tellurium compounds can be arranged as the following (according to the increase in their ionization potential) [18,37]:

D > **B** > **C** > **E**

Table 4. Electronegativity and electrophilicity of the organotellurium compounds

Compound	Electronegativity (X) (eV)	Electrophilicity (W) (eV)
$RTeBr_3$ (**B**)	4.1889	7.2209
R_2TeBr_2 (**C**)	3.4842	7.0538
R_2Te (**D**)	3.9345	14.0730
R_2Te_2 (**E**)	3.7671	5.8399

Table 5. Ionization potential and electron affinity of the organotellurium compounds

Compound	Ionization potential (I.P) (eV)	Electron affinity (E.A) (eV)
$RTeBr_3$ (**B**)	5.40	2.97
R_2TeBr_2 (**C**)	4.34	2.62
R_2Te (**D**)	4.48	3.38
R_2Te_2 (**E**)	4.98	2.55

Hardness Softness Acid Base

Chemical hardness is a very useful concept in chemistry and physics, knowing the resistance or deformation of atoms, molecules, or ions [40]. Based on this concept, was classified Lewis acids and bases were both hard and soft, and this principle was described by Pearson. A base can be defined as soft is the donor atom that is highly polarizable and has a low negative electronegativity. It is easily oxidized and bound to empty lower orbitals. As for the solid base, the donor atom is low polarizability, has high negative electronegativity, is easily oxidized, and is associated with empty orbitals with high energy, soft acid can be defined as the accepting atom with a positive charge. It is low, large, and polarizable. As for the solid acid, the receiving atom is the same high positive charge, small size, and non-polarizable. This principle includes a description of the behavior of molecules or atoms as acids and bases in chemistry. The soft base and the hard base represent the donors, but the soft acid the solid acid represents the acceptors. The following Eq. (6) and (7) can express the hardness and softness.

$$\eta = \frac{I.P - W.P}{2} \quad (6)$$

$$\sigma = \frac{1}{2\eta} \quad (7)$$

η refers to chemical hardness, and σ refers to chemical softness, from Table 6. The compound **D** was harder than compounds **B**, **C**, and **E**, respectively, indicating that compound D will behave as a hard base [40-42].

D > **C** > **E** > **B**

In addition, and from the information provided in Table 6, compound **D** appears softer than other compounds, while compound **B** behaves as a soft base. Therefore, organo-tellurium compounds are classified as donors or acceptors.

Table 6. Chemical hardness and chemical softness of the organotellurium compounds

Compound	Chemical hardness (η)	Chemical softness (σ)
$RTeBr_3$ (**B**)	1.215	0.4115
R_2TeBr_2 (**C**)	0.86	0.581
R_2Te (**D**)	0.55	0.9090
R_2Te_2 (**E**)	1.216	0.4116

■ CONCLUSION

In the present study, compounds **A**, **B**, **C**, **D**, and **E** were obtained in a 32–77% yield. All the prepared compounds were characterized by the mass spectrum and FTIR. Findings from this study were in concordance with previous research findings, confirming the correctness of the proposed structures for all the prepared compounds.

As for the theoretical study, it can be obtained that the DFT used in this study is an interest method, and the B3LYP functional is suitable for studying the electronic properties of these structures. The density functional theory method has been used for geometry optimization and the electronic properties of all prepared compounds by using B3LYP functional.

The total energies of the donor-acceptor system show that this structure is more stable. The results obtained in this work may help to select a type of bridge to interact with the donor and acceptor to calculate the physical properties of the donor-bridge-acceptor.

■ REFERENCES

[1] Liang, X., Perez, M.A.M.J., Nwoko, K.C., Egbers, P., Feldmann, J., Csetenyi, L., and Gadd, G.M., 2019, Fungal formation of selenium and tellurium nanoparticles, *Appl. Microbiol. Biotechnol.*, 103 (17), 7241–7259.

[2] Irfan, M., Rehman, R., Razali, M.R., Ur Rehman, S., Ur Rehman, A., and Iqbal, M.A., 2020, Organotellurium compounds: An overview of synthetic methodologies, *Rev. Inorg. Chem.*, 40 (4), 193–232.

[3] Chivers, T., and Laitinen, R.S., 2015, Tellurium: A maverick among the chalcogens, *Chem. Soc. Rev.*, 44 (7), 1725–1739.

[4] Pop, A., Silvestru, C., and Silvestru, A., 2019, Organoselenium and organotellurium compounds containing chalcogen-oxygen bonds in organic synthesis or related processes, *Phys. Sci. Rev.*, 4 (5), 20180061.

[5] Vaigankar, D.C., Dubey, S.K., Mujawar, S.Y., D'Costa, A., and Shyama, S.K., 2018, Tellurite biotransformation and detoxification by *Shewanella*

baltica with simultaneous synthesis of tellurium nanorods exhibiting photo-catalytic and anti-biofilm activity, *Ecotoxicol. Environ. Saf.*, 165, 516–526.

[6] Missen, O.P., Ram, R., Mills, S.J., Etschmann, B., Reith, F., Shuster, J., Smith, D.J., and Brugger, J., 2020, Love is in the earth: A review of tellurium (bio)geochemistry in surface environments, *Earth-Sci. Rev.*, 204, 103150.

[7] Alduino, C., Alfonso, K., Artusa, D.R., Avignone, F.T., Azzolini, O., Banks, T.I., Bari, G., Beeman, J.W., Bellini, F., Bersani, A., Biassoni, M., Brofferio, C., Bucci, C., Camacho, A., Caminata, A., Canonica, L., Cao, X.G., Capelli, S., Cappelli, L., Carbone, L., Cardani, L., Carniti, P., Casali, N., Cassina, L., Chiesa, D., Chott, N., Clemenza, M., Copello, S., Cosmelli, C., Cremonesi, O., Creswick, R.J., Cushman, J.S., D'Addabbo, A., Dafinei, I., Davis, C.J., Dell'Oro, S., Deninno, M.M., Di Domizio, S., Di Vacri, M.L., Drobizhev, A., Fang, D.Q., Faverzani, M., Feintzeig, J., Fernandes, G., Ferri, E., Ferroni, F., Fiorini, E., Franceschi, M.A., Freedman, S.J., Fujikawa, B.K., Giachero, A., Gironi, L., Giuliani, A., Gladstone, L., Gorla, P., Gotti, C., Gutierrez, T.D., Haller, E.E., Han, K., Hansen, E., Heeger, K.M., Hennings-Yeomans, R., Hickerson, K.P., Huang, H.Z., Kadel, R., Keppel, G., Kolomensky, Y.G., Leder, A., Ligi, C., Lim, K.E., Liu, X., Ma, Y.G., Maino, M., Marini, L., Martinez, M., Maruyama, R.H., Mei, Y., Moggi, N., Morganti, S., Mosteiro, P.J., Napolitano, T., Nones, C., Norman, E.B., Nucciotti, A., O'Donnell, T., Orio, F., Ouellet, J.L., Pagliarone, C.E., Pallavicini, M., Palmieri, V., Pattavina, L., Pavan, M., Pessina, G., Pettinacci, V., Piperno, G., Pira, C., Pirro, S., Pozzi, S., Previtali, E., Rosenfeld, C., Rusconi, C., Sangiorgio, S., Santone, D., Scielzo, N.D., Singh, V., Sisti, M., Smith, A.R., Taffarello, L., Tenconi, M., Terranova, F., Tomei, C., Trentalange, S., Vignati, M., Wagaarachchi, S.L., Wang, B.S., Wang, H.W., Wilson, J., Winslow, L.A., Wise, T., Woodcraft, A., Zanotti, L., Zhang, G.Q., Zhu, B.X., Zimmermann, S., and Zucchelli, S., 2017, Measurement of the two-neutrino double beta decay half-live of ^{130}Te with the CUORE-o experiment, *Eur. Phys. J. C*, 77 (1), 13.

[8] Clark, R.A., McNamara, B.K., Barinaga, C.J., Peterson, J.M., Govind, N., Andersen, A., Abrecht, D.G., Schwantes, J.M., and Ballou, N.E., 2015, Electron ionization mass spectrum of tellurium hexafluoride, *Inorg. Chem.*, 54 (10), 4821–4826.

[9] Sredni, B., 2012, Immunomodulating tellurium compounds as anti-cancer agents, *Semin. Cancer Biol.*, 22 (1), 60–69.

[10] Perron, J.C., 1967, Electrical and thermoelectrical properties of selenium-tellurium liquid alloys, *Adv. Phys.*, 16 (64), 657–666.

[11] Yin, Y., Cao, R., Guo, J., Liu, C., Li, J., Feng, X., Wang, H., Du, W., Qadir, A., Zhang, H., Ma, Y., Gao, S., Xu, Y., Shi, Y., Tong, L., and Dai, D., 2019, High-speed and high-responsivity hybrid silicon/black-phosphorus waveguide photodetectors at 2 μm, *Laser Photonics Rev.*, 13 (6), 1900032.

[12] Yamago, S., 2021, Practical synthesis of dendritic hyperbranched polymers by reversible deactivation radical polymerization, *Polym. J.*, 53 (8), 847–864.

[13] Kavlak, G., and Graedel, T.E., 2013, Global anthropogenic tellurium cycles for 1940–2010, *Resour., Conserv. Recycl.*, 76, 21–26.

[14] Filella, M., Reimann, C., Biver, M., Rodushkin, I., and Rodushkina, K., 2019, Tellurium in the environment: Current knowledge and identification of gaps, *Environ. Chem.*, 16 (4), 215–228.

[15] Aziz, F.K., Gazar, S.H., and Al-Saadawy, N.H., 2020, Simple, selective, and sensitive spectrophotometric method for determination of trace amounts of lead(II), cadmium(II), cobalt(II) with organomercury compounds, *J. Global Pharma Technol.*, 12 (6), 248–255.

[16] Al-Fregi, A.A., Al-Asfoor, A.F., and Jabar, S.F., 2015, Synthesis and characterization of some new series of 2-(4-hydroxynaphthylazo)-5-substituted phenyltellutrium tribromides and ditellurides compounds, *Int. J. Sci. Eng. Res.*, 6 (3), 274–281.

[17] Silverstein, R.M., and Bassler, G.C., 1962, Spectrometric identification of organic compounds, *J. Chem. Educ.*, 39 (11), 546.

[18] Oliveira, G.P., Barboza, B.H., and Batagin-Neto A., 2022, Polyaniline-based gas sensors: DFT study on

the effect of side groups, *Comput. Theor. Chem.*, 1207, 113526.

[19] Ahmed, W.M., Al-Saadawy, N.H., and Abowd, M.I., 2021, Synthesis and characterization of a new organoselenium and organotellurium compounds depending on 9-chloro-10-nitro-9,10-dihydroanthracene, *Ann. Romanian Soc. Cell Biol.*, 25 (4), 11035–11043.

[20] Anand, D., He, Y., Li, L., and Zhou, L., 2019, A photocatalytic sp^3 C–S, C–Se and C–B bond formation through C–C bond cleavage of cycloketone oxime esters, *Org. Biomol. Chem.*, 17 (3), 533–540.

[21] Pavia, D.L., Lampman, G.M., Kriz, G.S., and Vyvyan, J.A., 2014, *Introduction to Spectroscopy*, Cengage Learning, Boston, US.

[22] Al-Saadawy, N.H., 2022, New organotellurium compounds based on camphor, aniline and *p*-toluidine: Preparation, characterization and theoretical study, *Egypt. J. Chem.*, 65 (2), 19–27.

[23] Abbas, S.H., Al-Fregi, A.A., and Al-Yaseen, A.A., 2021, Synthesis of some new organotellurium compounds based on 1-substituted tetrazole, *J. Phys.: Conf. Ser.*, 1853, 012034.

[24] McWhinnie, W.R., and Thavornyutikarn, P., 1972, A spectroscopic examination of phenyltellurium trihalides, *J. Chem. Soc., Dalton Trans.*, 4, 551–554.

[25] Boursas, F., Berrah, F., Kanagathara, N., Anbalagan, G., and Bouacida, S., 2019, XRD, FT-IR, FT-Raman spectrum and ab initio HF vibrational analysis of bis (5-amino-3-carboxy-1*H*-1,2,4-triazol-4-ium) selenate dihydrate, *J. Mol. Struct.*, 1180, 532–541.

[26] Khanage, S.G., 2014, Synthesis and biological evaluation of new triazole derivatives, *Dissertation*, Vinayaka Missions University, Tamil Nadu, India.

[27] Abdul-Nabi, A.S., and Jasim, E.Q., 2014, Synthesis, characterization and study of some tetrazole compounds as new corrosion inhibitors for C-steel in 0.5 M HCl solution, *Int. J. Eng. Res.*, 3 (10), 613–617.

[28] Scheinmann, F., 2013, *An Introduction to Spectroscopic Methods for the Identification of Organic Compounds: Mass Spectrometry, Ultraviolet Spectroscopy, Electron Spin Resonance Spectroscopy, Nuclear Magnetic Resonance Spectroscopy (Recent Developments), Use of Various Spectral Methods Together, and Documentation of Molecular Spectra*, Elsevier Science, Amsterdam, Netherlands.

[29] Al-Rubaie, A.Z., and Yousif, L.Z., 2020, Synthesis and reaction of 2-acetylamino-2'-tellurocyanato-1,1'-binaphthyl, *IOP Conf. Ser.: Mater. Sci. Eng.*, 928, 52035.

[30] Achouba, A., Dumas, P., Ouellet, N., Little, M., Lemire, M., and Ayotte, P., 2019, Selenoneine is a major selenium species in beluga skin and red blood cells of Inuit from Nunavik, *Chemosphere*, 229, 549–558.

[31] Frogley, B.J., Genet, T.L., Hill, A.F., and Onn, C.S., 2019, Alkynylselenolatoalkylidynes ($L_nM{\equiv}C{-}Se{-}C{\equiv}CR$) as building blocks for mixed metal/main-group extended frameworks, *Dalton Trans.*, 48 (22), 7632–7643.

[32] Al-Asadi, R.H., 2019, Synthesis, DFT calculation and biological activity of some organotellurium compounds containing azomethine group, *Orbital: Electron. J. Chem.*, 11 (7), 402–410.

[33] Gusakova, J., Wang, X., Shiau, L.L., Krivosheeva, A., Shaposhnikov, V., Borisenko, V., Gusakov, V., and Tay, B.K., 2017, Electronic properties of bulk and monolayer TMDs: Theoretical study within DFT framework (GVJ-2e method), *Phys. Status Solidi A*, 214 (12), 1700218.

[34] Bagayoko, D., 2014, Understanding density functional theory (DFT) and completing it in practice, *AIP Adv.*, 4 (12), 127104.

[35] Koch, W., and Holthausen, M.C., 2015, *A Chemist's Guide to Density Functional Theory*, Wiley-VCH, Weinheim, Germany.

[36] Ali, A.M., 2009, Investigations of some antioxidant materials by using density functional and semiempirical theories, *Dissertation*, College of Science, University of Basrah, Iraq.

[37] Sheela, N.R., Muthu, S., and Sampathkrishnan, S., 2014, Molecular orbital studies (hardness, chemical potential, and electrophilicity), vibrational investigation and theoretical NBO analysis of 4-4′-(1H-1,2,4-triazol-1-yl methylene) dibenzonitrile

based on *ab initio* and DFT methods, *Spectrochim. Acta, Part A*, 120, 237–251.

[38] Arivazhagan, M., Manivel, S., Jeyavijayan, S., and Meenakshi, R., 2015, Vibrational spectroscopic (FTIR and FT-Raman), first-order hyperpolarizablity, HOMO, LUMO, NBO, Mulliken charge analyses of 2-ethylimidazole based on Hartree–Fock and DFT calculations, *Spectrochim. Acta, Part A*, 134, 493–501.

[39] Al-Saadawy, N.H., 2022, Synthesis, characterization, and theoretical study of some new organotellurium compounds derived from camphor, *Indones. J. Chem.*, 22 (2), 437–448.

[40] Abood, H.I., 2014, Density functional theory calculations of di-amino naphthalene, *J. Univ. Babylon Pure Appl. Sci.*, 22 (3), 1132–1145.

[41] Vikramaditya, T., and Lin, S.T., 2017, Assessing the role of Hartree Fock exchange, correlation energy and long range corrections in evaluating ionization potential, and electron affinity in density functional theory, *J. Comput. Chem.*, 38 (21), 1844–1852.

[42] Kaya, S., Kariper, S.E., Ungördü, A., and Kaya, C., 2014, Effect of some electron donor and electron acceptor groups on stability of complexes according to the principle of HSAB, *J New Results Sci.*, 4, 82–89.

[43] Vennila, P., Govindaraju, M., Venkatesh, G., and Kamal, C., 2016, Molecular structure, vibrational spectral assignments (FT-IR and FT-RAMAN), NMR, NBO, HOMO-LUMO and NLO properties of O-methoxybenzaldehyde based on DFT calculations, *J. Mol. Struct.*, 1111, 151–156.

Supplementary Data

This supplementary data is a part of a paper entitled "Synthesis, Characterization, and Theoretical Study of a New Organotellurium Ligands Containing Amino Group".

The spectra details (FT-IR and MS) of the prepared organotellurium compounds

(4-Amino-[1,1'-biphenyl]-3-yl)mercury(II) chloride (A): -

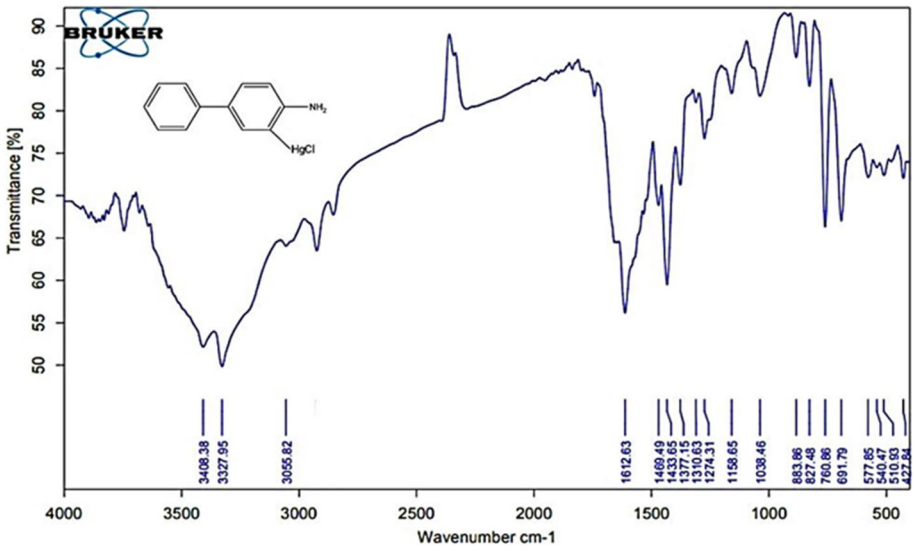

Fig S1. Infrared spectrum of the compound **A**

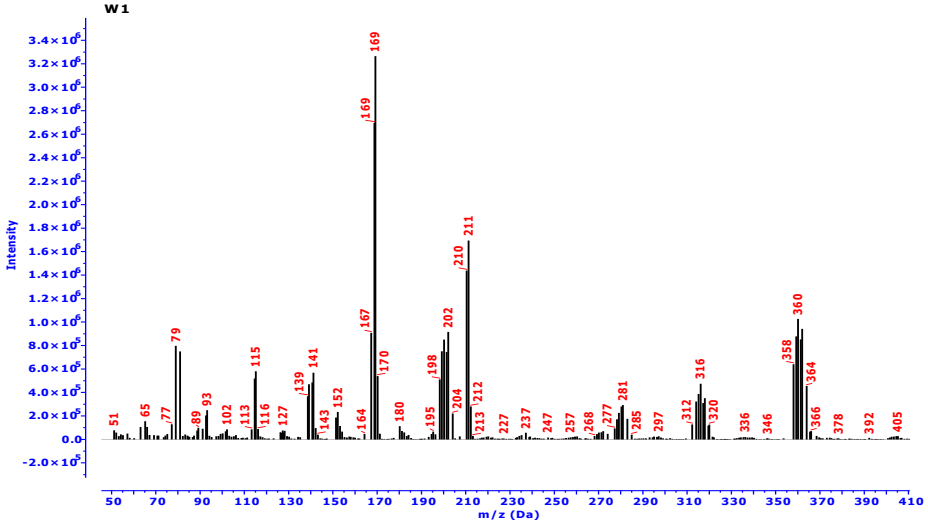

Fig S2. The mass spectrum of the compound **A**

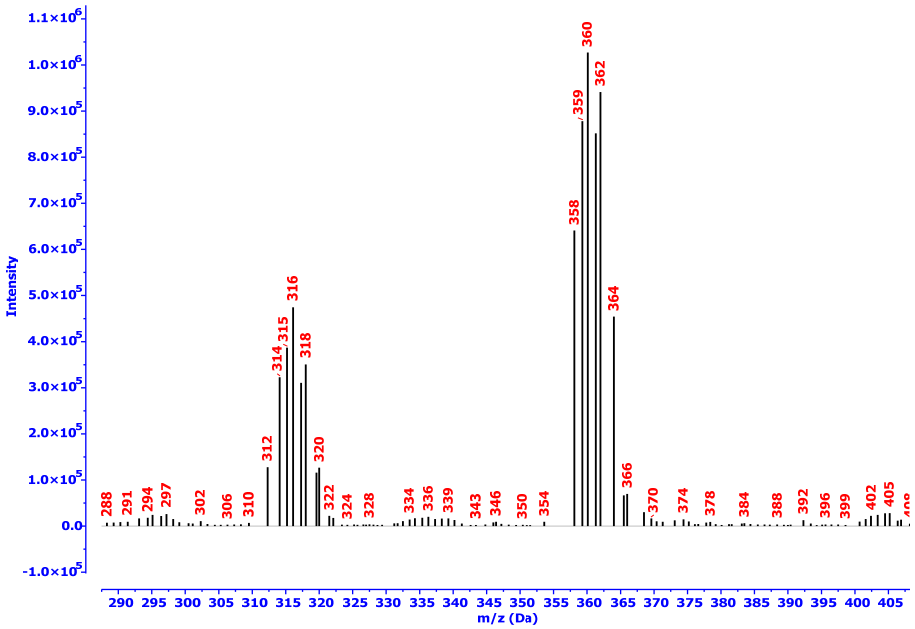

Fig S3. Expanded mass spectrum of the compound **A**

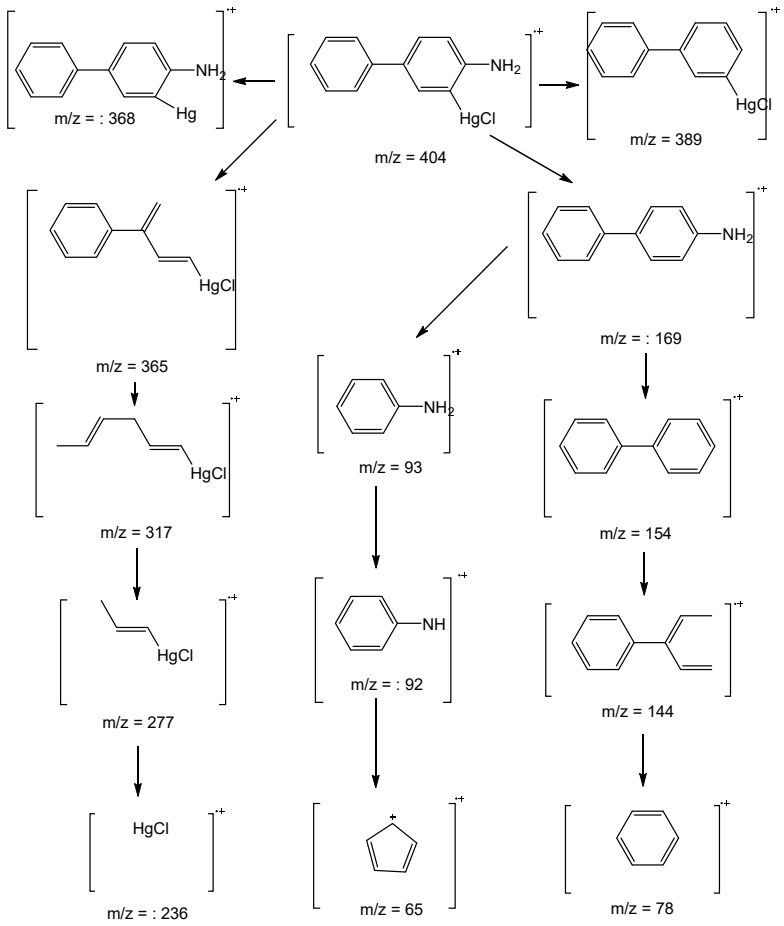

Scheme S1. Mechanical fragmentation of the compound **A**

3-(Tribromo-λ^4-tellanyl)-[1,1'-biphenyl]-4-amine (B): -

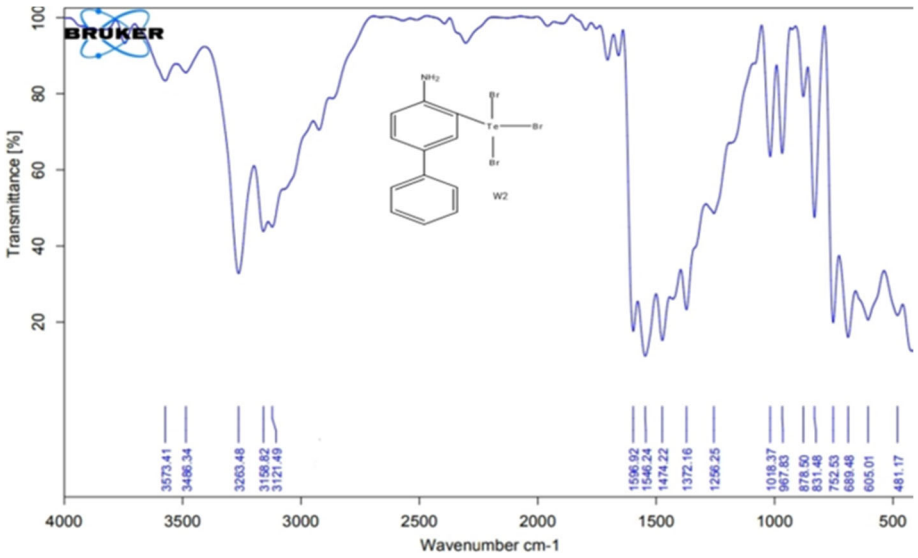

Fig S4. Infrared spectrum of the compound **B**

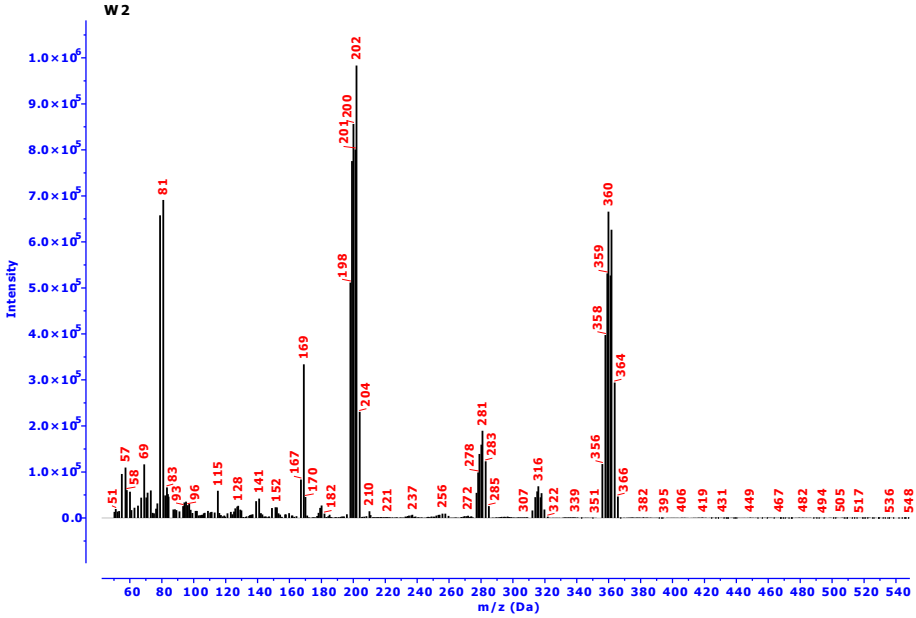

Fig S5. The mass spectrum of the compound **B**

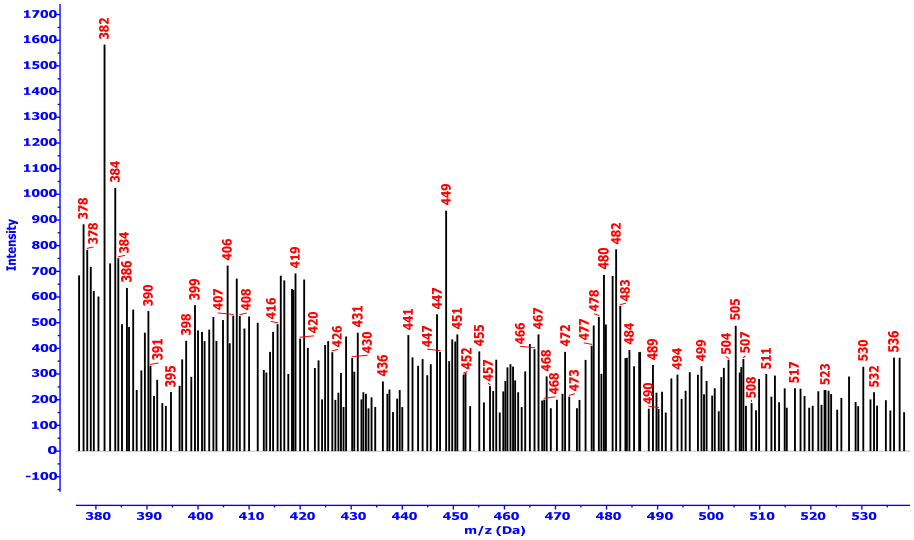

Fig S6. Expanded mass spectrum of the compound **B**

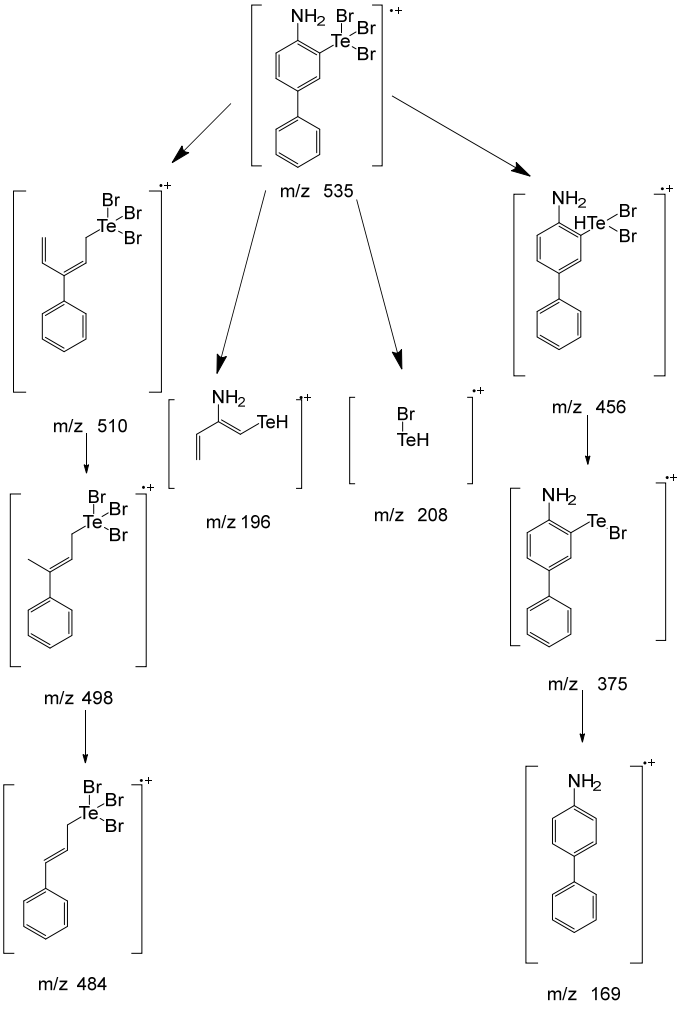

Scheme S2. Mechanical fragmentation of the compound **B**

3,3'-(Dibromo-λ^4-tellanediyl)bis([1,1'-biphenyl]-4-amine) (C): -

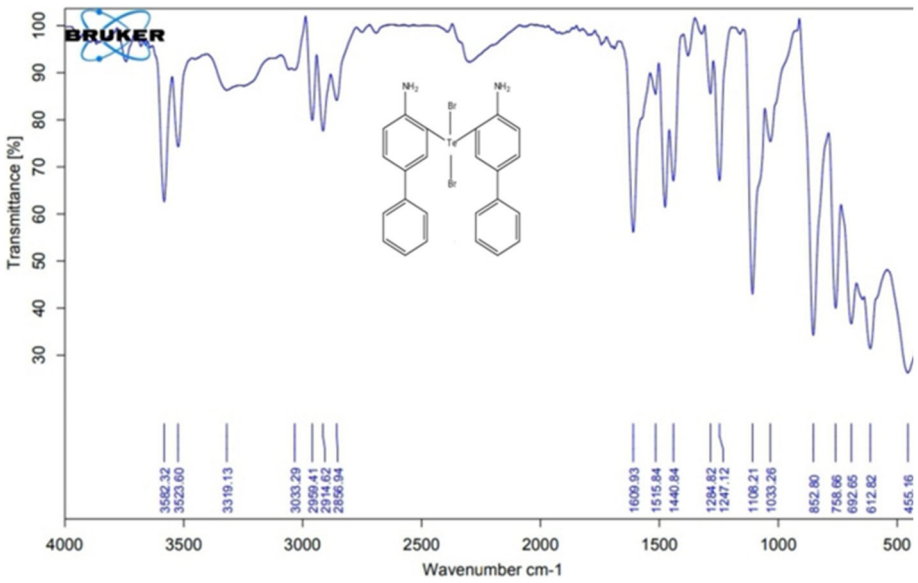

Fig S7. Infrared spectrum of the compound **C**

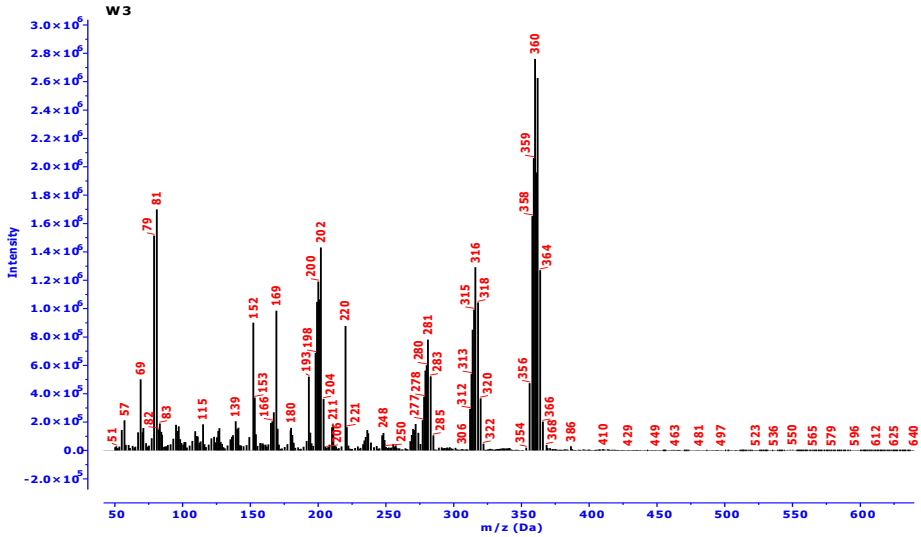

Fig S8. The mass spectrum of the compound **C**

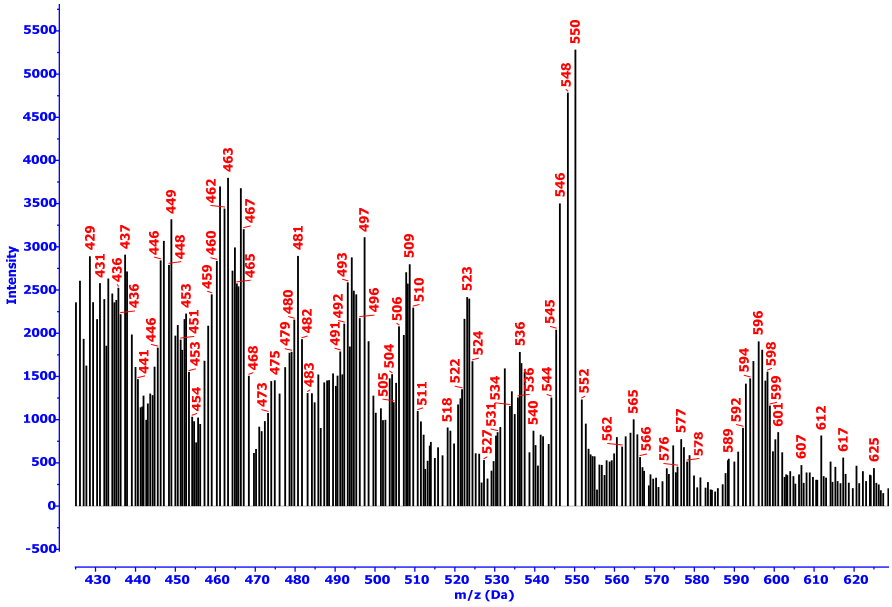

Fig S9. Expanded mass spectrum of the compound **C**

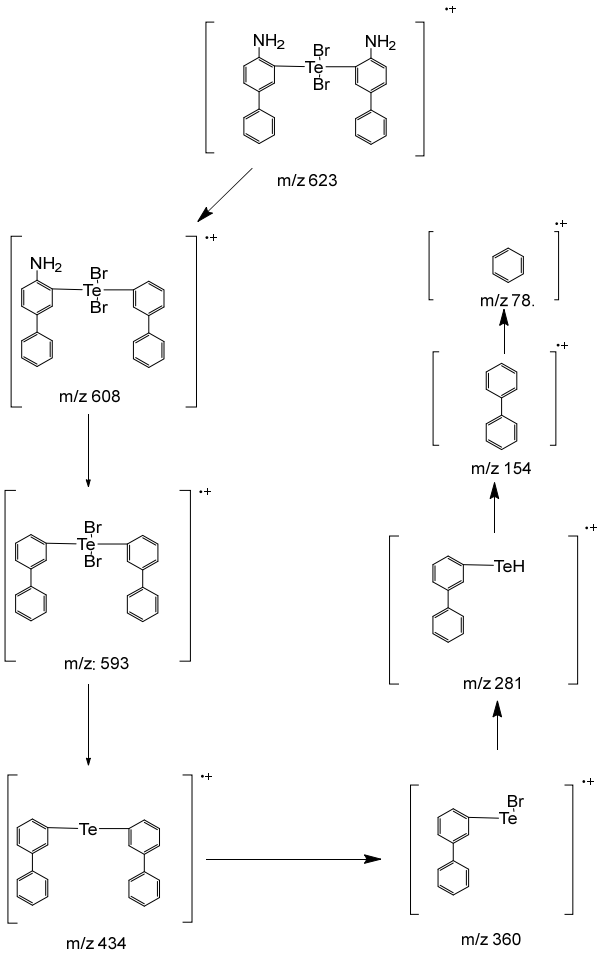

Scheme S3. Mechanical fragmentation of the compound **C**

3,3''-tellurobis([1,1'-biphenyl]-4-amine) (D): -

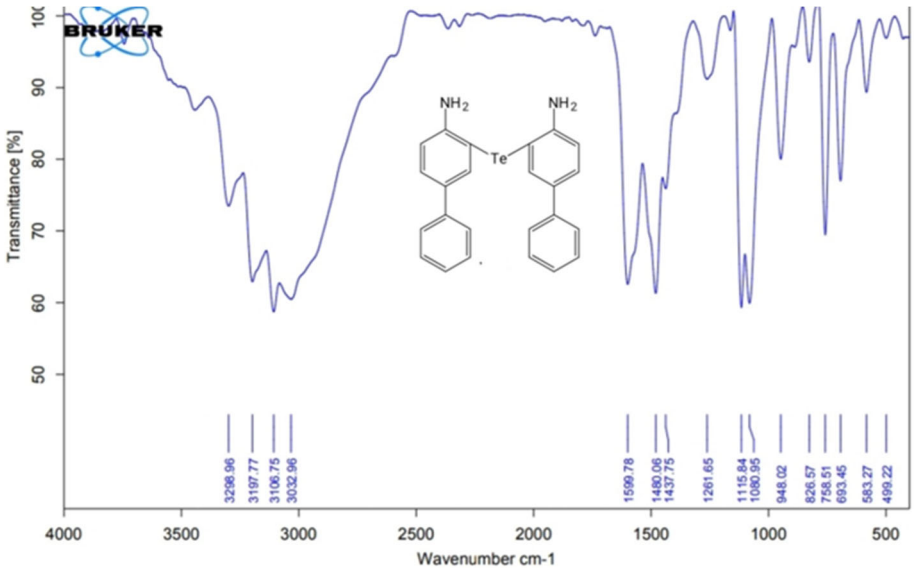

Fig S10. Infrared spectrum of the compound **D**

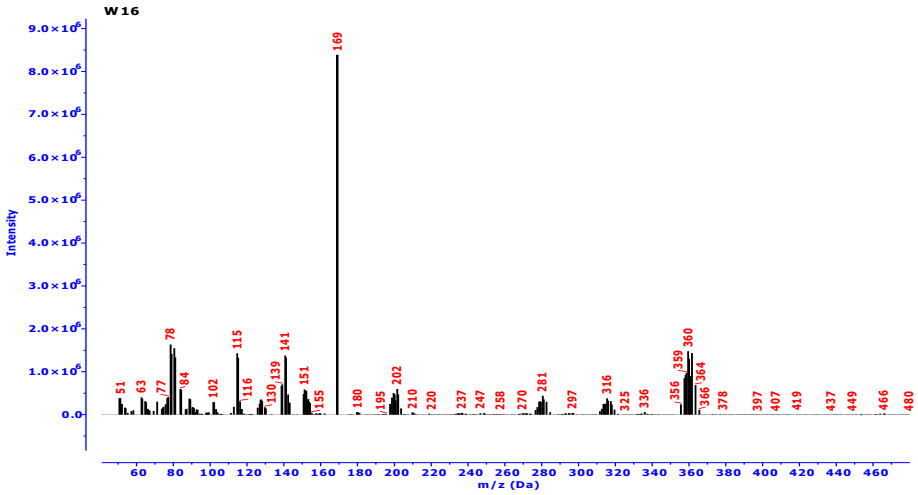

Fig S11. The mass spectrum of the compound **D**

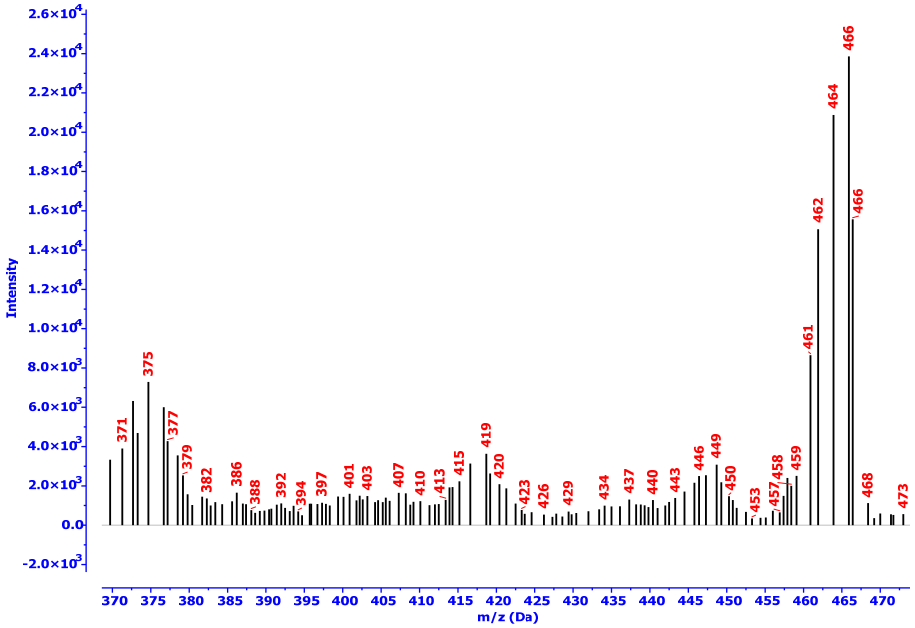

Fig S12. Expanded mass spectrum of the compound **D**

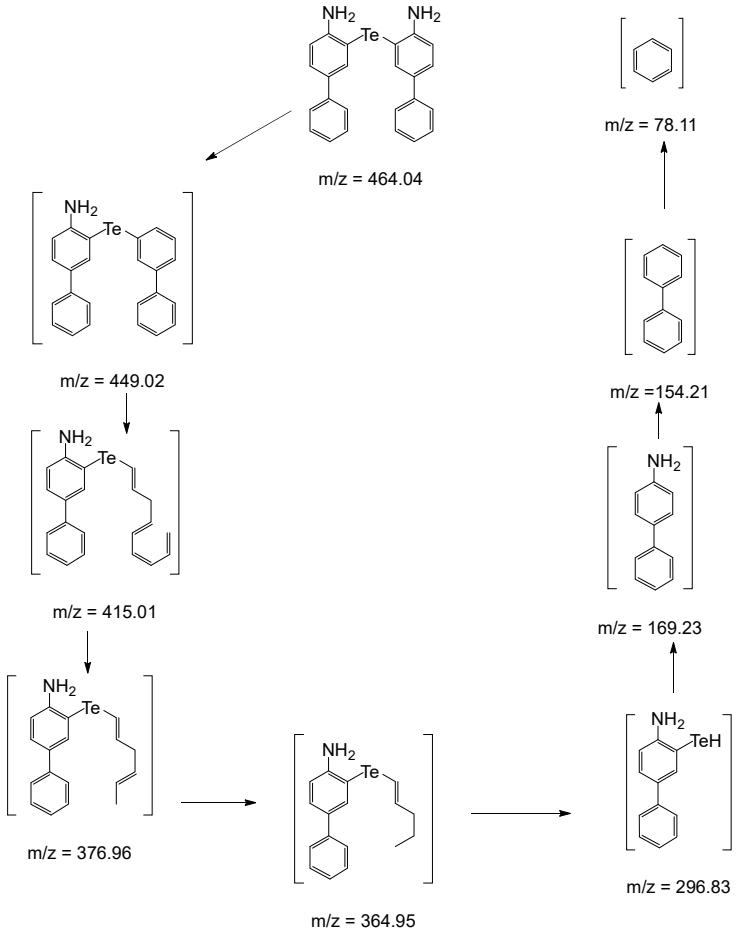

Scheme S4. Mechanical fragmentation of the compound **D**

3,3''-ditellanediyl bis([1,1'-biphenyl]-4-amine) (E): -

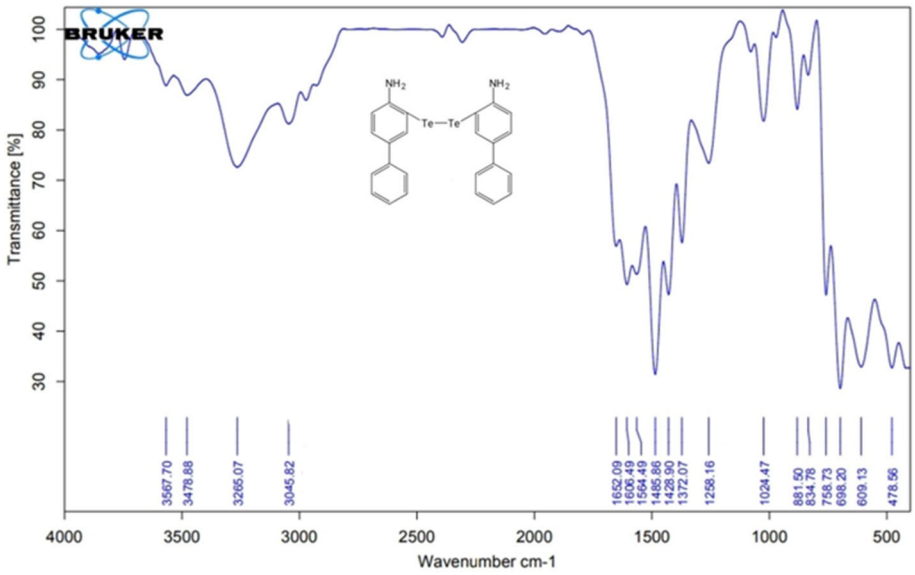

Fig S13. Infrared spectrum of the compound **E**

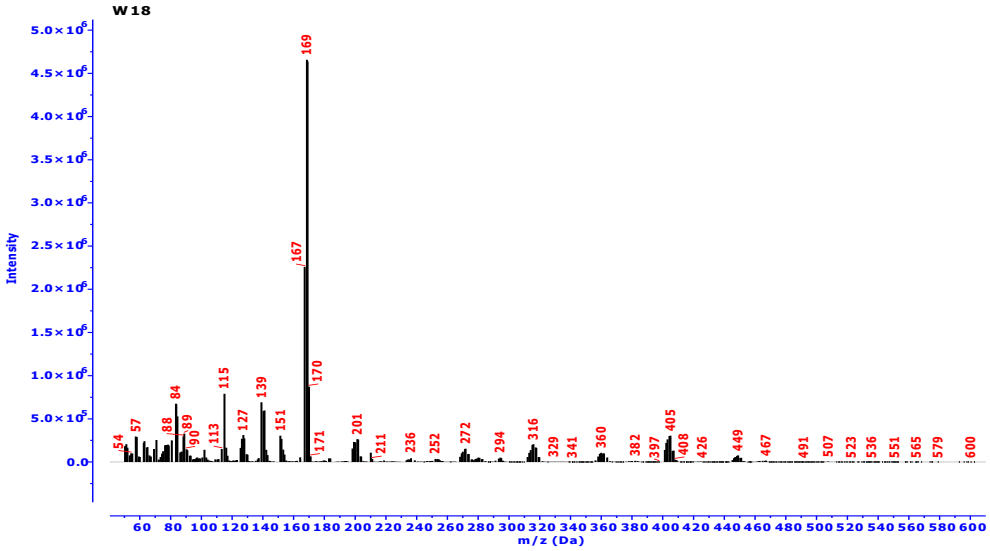

Fig S14. The mass spectrum of the compound **E**

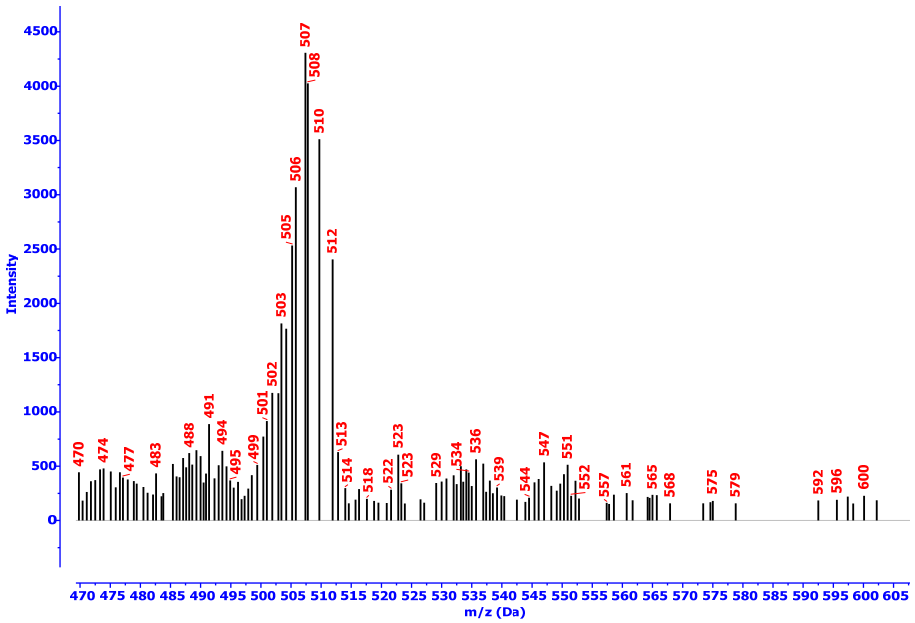

Fig S15. Expanded mass spectrum of the compound **E**

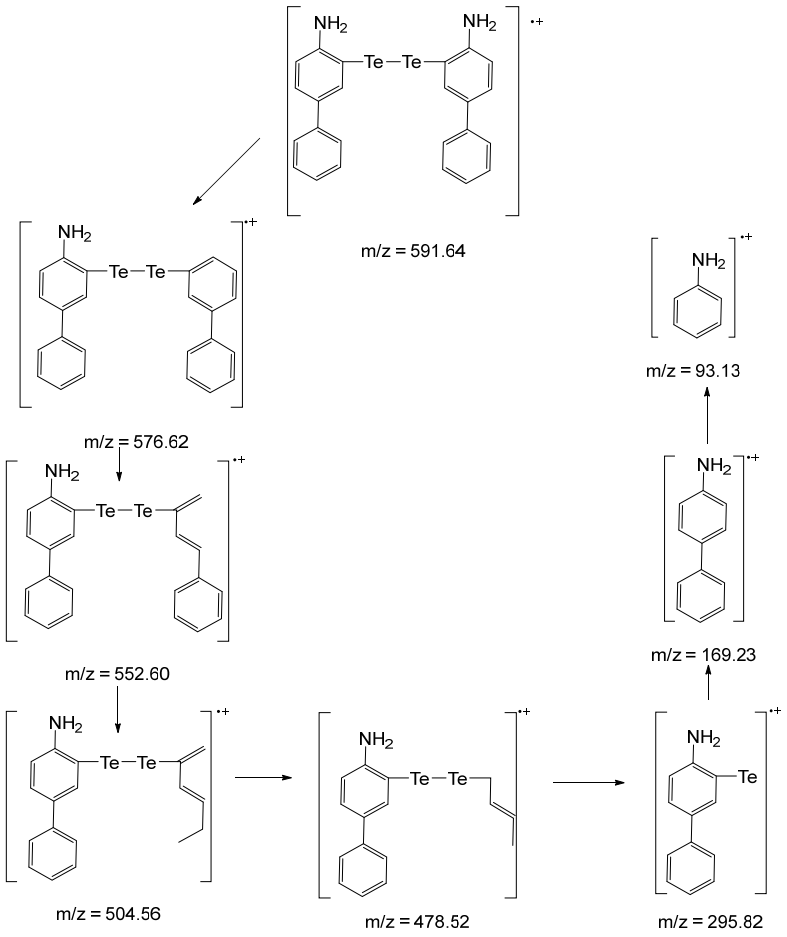

Scheme S5. Mechanical fragmentation of the compound **E**

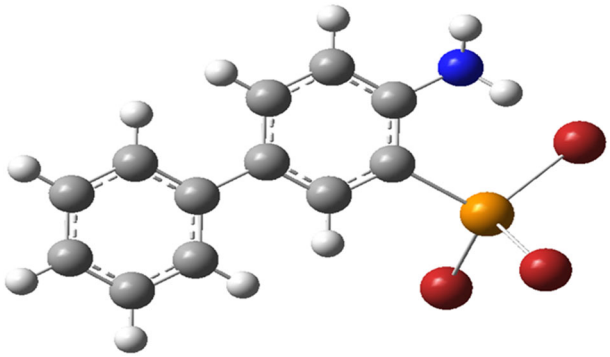

Fig S16. Molecular structure of compound **B**

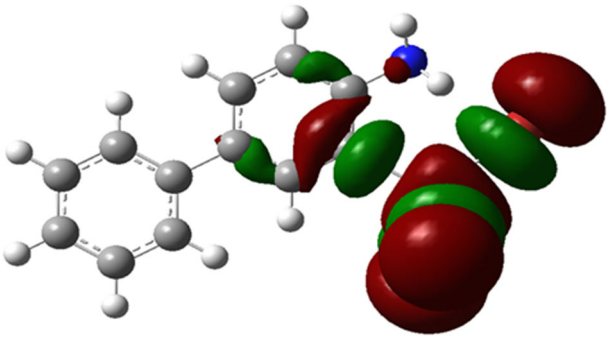

Fig S17. Molecular orbital (HOMO) of compound **B**

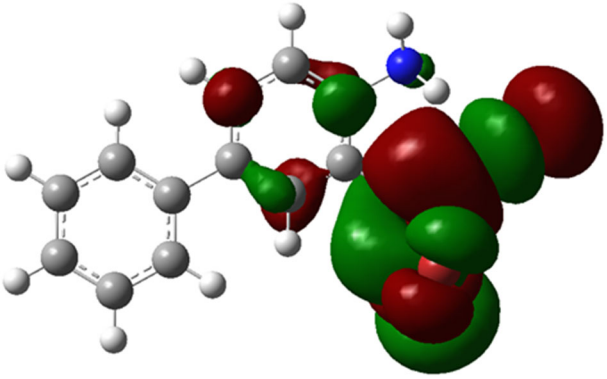

Fig S18. Molecular orbital (LUMO) of compound **C**

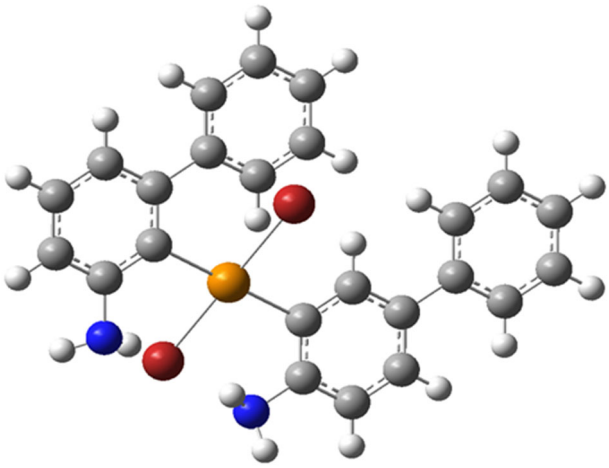

Fig S19. Molecular structure of compound **C**

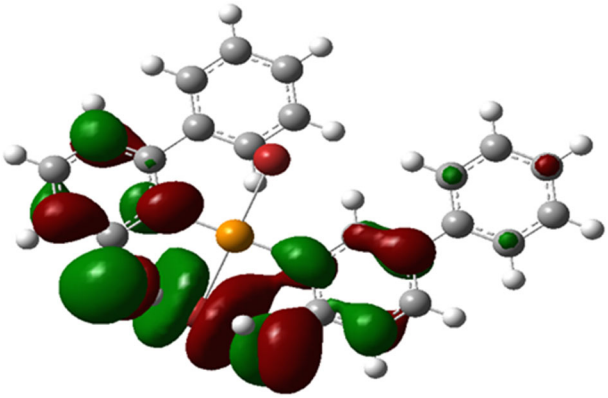

Fig S20. Molecular orbital (HOMO) of compound **C**

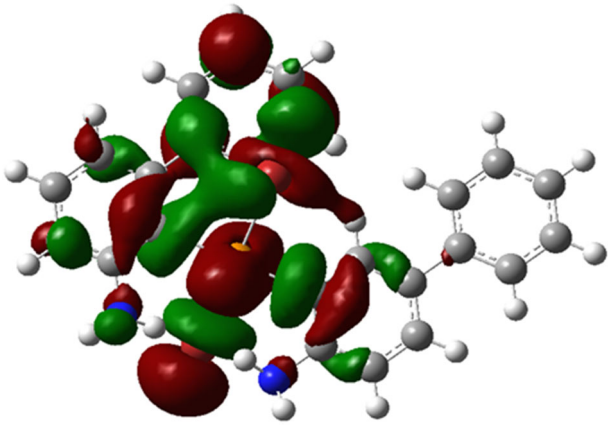

Fig S21. Molecular orbital (LUMO) of compound **C**

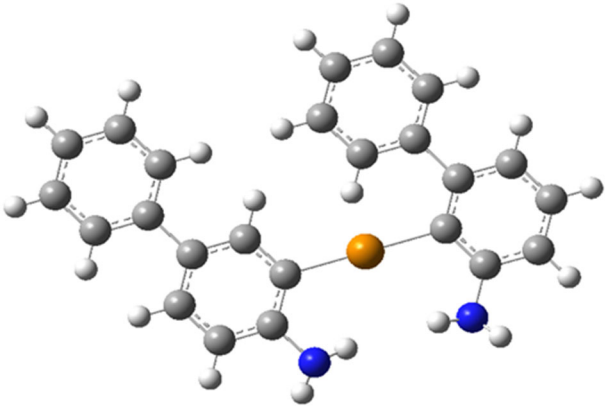

Fig S22. Molecular structure of compound **D**

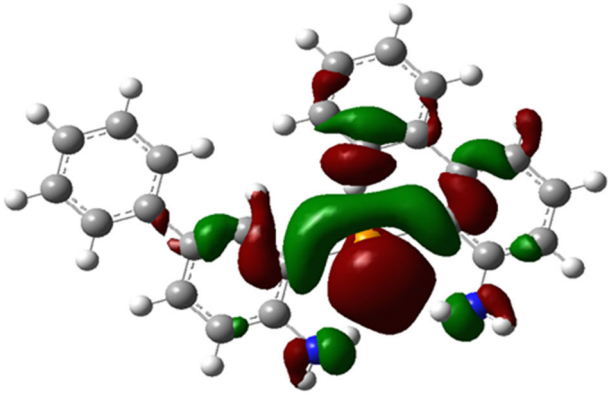

Fig S23. Molecular orbital (HOMO) of compound **D**

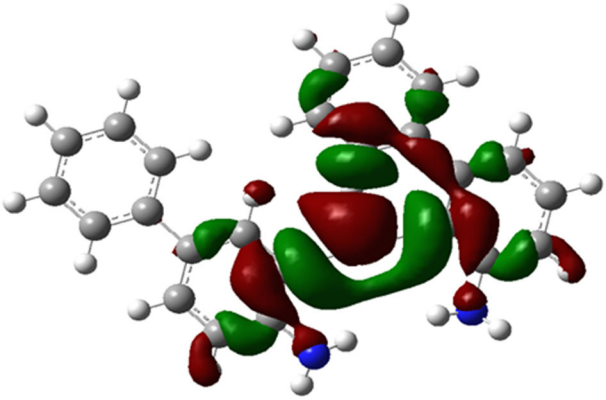

Fig S24. Molecular orbital (LUMO) of compound **D**

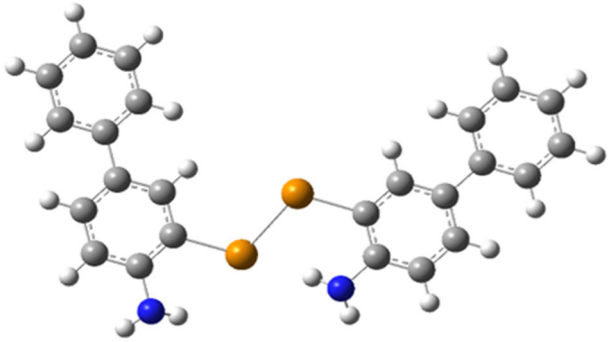

Fig S25. Molecular structure of compound **E**

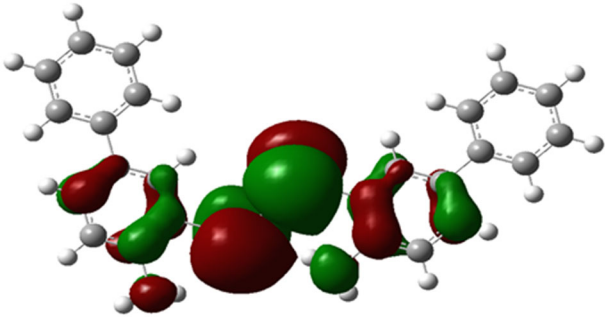

Fig 26. Molecular orbital (HOMO) of compound **E**

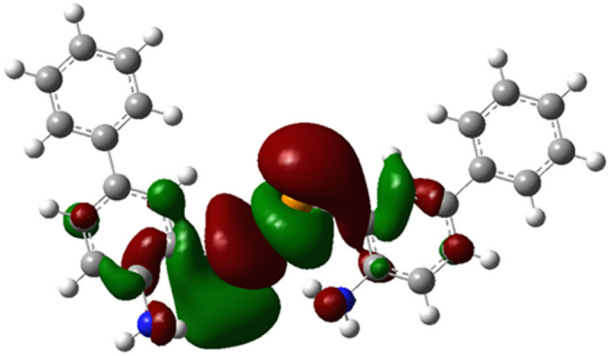

Fig S27. Molecular orbital (LUMO) of compound **E**

Table S1. The most important fissions of the compound **A**

Molecular ion	*m/z*	Molecular ion	*m/z*
$[C_{12}H_{10}NHgCl]^+$	404	$[C_6H_9HgCl]^+$	317
$[C12H11N]^+$	169	$[C_{12}H_{10}]^+$	154
$[C_{10}H_9HgCl]^+$	365	$[C_3H_5HgCl]^+$	277

Table S2. The most important fissions of the compound **B**

Molecular ion	*m/z*	Molecular ion	*m/z*
$[C_{12}H_{10}Br_3NTe]^+$	535	$[C_4H_7NTe]^+$	196
$[TeHBr]^+$	202	$[C_{12}H_{11}Br_2NTe]^+$	456
$[C_{11}H_{11}Br_3Te]^+$	510	$[C_{12}H_{11}N]^+$	169

Table S3. The most important fissions of the compound **C**

Molecular ion	*m/z*	Molecular ion	*m/z*
$[C_{24}H_{20}N_2Br_2Te]^+$	623	$[C_{24}H_{18}Br_2Te]^+$	593
$[C_{12}H_9BrTe]^+$	360	$[C_{24}H_{18}Te]^+$	434
$[C_{24}H_{19}Br_2NTe]^+$	608	$[C_{12}H_{10}Te]^+$	281

Table S4. The most important fissions of the compound **D**

Molecular ion	*m/z*	Molecular ion	*m/z*
$[C_{24}H_{20}N_2Te]^+$	464	$[C_{21}H_{21}NTe]^+$	415
$[C_{12}H_{11}N]^+$	169	$[C_{17}H_{19}NTe]^+$	364
$[C_{24}H_{19}NTe]^+$	449	$[C_6H_6]^+$	77

Table S5. The most important fissions of the compound **E**

Molecular ion	*m/z*	Molecular ion	*m/z*
$[C_{24}H_{20}N_2Te_2]^+$	591	$[C_{22}H_{19}NTe_2]^+$	552
$[C_{12}H_{11}N]^+$	169	$[C_{12}H_{10}NTe]^+$	296
$[C_{24}H_{19}NTe_2]^+$	576	$[C_6H_7N]^+$	93